

Submicroscopic Deletion in Patients with Williams-Beuren Syndrome Influences Expression Levels of the Nonhemizygous Flanking Genes

Giuseppe Merla, Cédric Howald, Charlotte N. Henrichsen, Robert Lyle, Carine Wyss, Marie-Thérèse Zobot, Stylianos E. Antonarakis, and Alexandre Reymond

Genomic imbalance is a common cause of phenotypic abnormalities. We measured the relative expression level of genes that map within the microdeletion that causes Williams-Beuren syndrome and within its flanking regions. We found, unexpectedly, that not only hemizygous genes but also normal-copy neighboring genes show decreased relative levels of expression. Our results suggest that not only the aneuploid genes but also the flanking genes that map several megabases away from a genomic rearrangement should be considered possible contributors to the phenotypic variation in genomic disorders.

Segmental aneuploidies (i.e., gain or loss of subchromosomal DNA fragments) are important contributors to human diseases¹ and, potentially, to phenotypic variation,^{2,3} as well as a major force of evolutionary changes.⁴⁻⁹ There is evidence that such genomic insertions and deletions contribute to phenotypic differences by modifying the expression levels of genes within the aneuploid segments.¹⁰⁻¹³ We hypothesize that these rearrangements also induce altered expression of the genes that lie near the breakpoints, although these do not vary in copy number; this effect could be mediated by disturbances of the copy number of long-range *cis* regulatory elements.¹⁴⁻¹⁷

To test this hypothesis, we assessed whether the human chromosome 7 (HSA7) recurrent DNA deletion causing Williams-Beuren syndrome (WBS [MIM 194050])¹⁸ influences the transcription levels of both the hemizygous genes within the deleted region and the nonhemizygous genes in the WBS flanking regions. WBS is a neurodevelopmental disorder characterized by numerous clinical aspects, including mental retardation with a unique cognitive and personality profile.¹⁹ Its incidence is estimated to be between 1:7,500 and 1:20,000, and sporadic *de novo* inheritance is usual.²⁰⁻²²

Material and Methods

Cell Culture, RNA, and cDNA Preparations

Human skin fibroblasts and lymphoblastoid cell lines were grown in HAM F-10 or RPMI 1640 media, respectively, supplemented with 10% fetal bovine serum and 1% antibiotics (Invitrogen). Total RNA was prepared from logarithmic growth-phase cells, with the use of RNeasy Mini Kit (Qiagen), in accordance with the manufacturer's instructions. After DNase treatment (Qiagen), the quality of all RNA samples were checked using an Agilent 2100

Bioanalyzer (Agilent Technologies). Total RNA was converted to cDNA with the use of Superscript II (Invitrogen) primed with poly d(T). For each cell line included in the study, 4.5 μ g of total RNA was converted to cDNA in three individual reactions; these were then pooled and were diluted 1:14.

Sample Population

Lymphoblastoid cell lines from 10 individuals with WBS and from 40 control individuals, as well as skin fibroblasts from 7 control individuals, were acquired from the cell culture collection of the Coriell Institute for Medical Research, and skin fibroblasts from 14 individuals with WBS and from 6 control individuals were obtained from the cell culture collections of the Centre de Biotechnologie Cellulaire, Hospices Civils de Lyon, Hôpital Debrousse, in Lyon, France. One more control was received from the Galliera Genetic Bank in Genova, Italy (table 1). Appropriate informed consent was obtained for each sample by the physicians in charge. DNA was extracted from each cell line of the sample population, with the use of PureGene (Gentra Systems), in accordance with the manufacturer's instructions. We assayed each DNA with a quantitative PCR approach, using SybrGreen dye and probes, mapping the region from the *BAZ1* locus to the *CYLN2* locus and the flanks of the commonly deleted region,²³ to determine the size of the deletions and to ensure (1) that none of the patients with WBS presented an atypical deletion²³⁻²⁹ or an inversion at 7q11.23^{18,30} and (2) that none of the controls were hemizygous for that same region. The results are presented in table 2.

To make sure that differences in expression levels measured in lymphoblastoid cells were not merely due to transformation, we established six lymphoblastoid cell lines from two blood samples collected at 1-wk intervals from the same individual, after informed consent. We measured expression levels of 25 HSA21 genes (*ITBG2*, *CBS*, *APP*, *PFKL*, *U2AF1*, *PRDM15*, *LSS*, *PDXK*, *SLC19A1*, *SLC37A1*, *PWP2H*, *MCM3AP*, *GART*, *CBR1*, *TMEM1*,

From the Department of Genetic Medicine and Development, University of Geneva Medical School, Geneva, Switzerland (G.M.; C.H.; R.L.; C.W.; S.E.A.; A.R.); Servizio Genetica Medica, IRCCS Casa Sollievo della Sofferenza, San Giovanni Rotondo, Italy (G.M.); Centre de Biotechnologie Cellulaire, Hospices Civils de Lyon, Hôpital Debrousse (M.-T.Z.), and Interdisciplinary Group to Study the *ELN* Gene (M.-T.Z.), Lyon, France; and Center for Integrative Genomics, University of Lausanne, Lausanne, Switzerland (C.N.H.; A.R.)

Received April 26, 2006; accepted for publication May 31, 2006; electronically published June 23, 2006.

Address for correspondence and reprints: Dr. Alexandre Reymond, Center for Integrative Genomics, Genopode Building, University of Lausanne, Lausanne, Switzerland. E-mail: alexandre.reymond@unil.ch

Am. J. Hum. Genet. 2006;79:332-341. © 2006 by The American Society of Human Genetics. All rights reserved. 0002-9297/2006/7902-0015\$15.00

Table 1. Cell Lines Employed

The table is available in its entirety in the online edition of *The American Journal of Human Genetics*.

BTG3, *DSCR1*, *ETS2*, *IFNAR2*, *ANKRD3*, *WRB*, *GABPA*, *SON*, *IFNARI*, and *CCT8*) that show a large variation in transcript levels in the normal population and found no significant differences in their expression levels in the assayed samples (Pearson $0.8 < r < 0.92$ [mean 0.87]; $P < .001$). The observed differences correspond to the experimental variation we measure between replicates.

Real-Time Quantitative PCR and Data Analysis

We opted for Taqman real-time quantitative PCR, to measure any small differences in gene expression levels. Primers and probes were designed using the PrimerExpress program (Applied Biosystems), with default parameters in every case for all the confirmed genes mapping on HSA7, from the centromere to the beginning of band 7q21.11. They can be divided into three groups of genes: 23 HSA7 test genes that are hemizygous in patients with WBS, 2 genes mapping in the low-copy repeats (LCRs) flanking the WBS deletion, and 24 HSA7 test genes that are nonhemizygous in patients with WBS. We also designed assays in 2 HSA7p genes, in 13 control genes, and in 3 normalization genes. The complete list of tested genes, their accession numbers and mapping positions, and the primers and probes used are indicated in table 3. Amplicon sequences were checked by both BLAST and BLAT against the human genome, to ensure specificity. Whenever possible (in 94% of cases), oligos were designed to span an intron. Non-intron-spanning assays were tested in standard \pm reverse transcriptase reactions of RNA samples for genomic contamination; in all cases, no amplification was observed in the absence of reverse transcriptase. High-performance liquid chromatography-purified, FAM-TAMRA-labeled, double-dye Taqman probes and qPCR mastermix (RT-QP2X-03) were obtained from Eurogentec.

The efficiency of each Taqman assay was measured using a dilution series of fibroblast cDNA and lymphoblastoid cells or a pool of cDNA samples of brain, liver, and testis, as described elsewhere³¹ (see table 3 for results). A working Taqman assay was obtained for 57 (85%) of the 67 assayed genes. We were unsuccessful for *RCP9*, *RABGEF1*, *FKBP6*, *FZD9*, *WBSCR14*, *CLDN4*, *MK-STYX*, *FGL2*, *AIP*, and *GRM3*. Six more genes (*TPST1*, *WBSCR17/GALNT9*, *CALN1*, *WBSCR27*, *WBSCR28*, and *WBSCR16*) were excluded because of a lack of expression in both fibroblasts and lymphoblastoid cell lines (see efficiencies in table 3). Note that *TRIM50/73/74*, *ATP50*, *SIM2*, and *UFD1L* are not expressed in skin fibroblasts, whereas *WBSCR24*, *WBSCR18*, *CLDN3*, *ELN*, *CACNA2D1*, *GABPA*, *IFNGR2*, and *DGCR8* are not expressed in lymphoblastoids. Thus, in at least one of the two studied cell lines, we were able to assess the relative expression level (REL) of 76% (51/76) of the selected genes, a proportion significantly above the one expected with genomewide technologies. Typically, microarrays hybridized with fibroblast or lymphoblastoid cell cDNA measure the expression of 30%–40% of human genes.

All RT-PCRs were performed in a 10- μ l final volume and in five

Table 2. Genotyping of Cell Lines

The table is available in its entirety in the online edition of *The American Journal of Human Genetics*.

Table 3. Assayed Genes, Primers, Probes, and Efficiencies

The table is available in its entirety in the online edition of *The American Journal of Human Genetics*.

replicates per sample and were set up in a 384-well plate format, with the use of a Biomek 2000 robot (Beckman). They were run in an ABI 7900 Sequence Detection System (Applied Biosystems) with the following amplification conditions: 50°C for 2 min, 95°C for 10 min, and 50 cycles at 95°C for 15 s and 60°C for 1 min. Each plate contained the appropriate normalization genes to control for any variability between the different plate runs.

Raw threshold-cycle (C_t) values were obtained using SDS2.2 (Applied Biosystems). To calculate the normalized relative expression ratio between individuals with WBS and controls, we followed methods described elsewhere.³¹ We exploited the ge-Norm method³² to select the three normalization genes: *AGPAT1*, *EEF1A1*, and *PSMAS*. They were used to normalize input cDNA for each sample, whereas mixes of 40 lymphoblastoid and 12 fibroblast control-cell-line cDNA samples (table 1) were used to define normal RELs.

Results

We used the high sensitivity of real-time quantitative PCR to accurately measure the expression of all the HSA7q genes mapping in the region 11.9 Mb downstream (band 7q21.11) to 8.4 Mb upstream (centromere position) of the WBS deleted region, in which we could design a working Taqman assay (i.e., efficiency ≥ 0.95 and ≤ 1.05 for expression in fibroblasts and/or lymphoblastoid cell lines) (see “Material and Methods” and table 3 for details). These genes can be divided into 17 HSA7q hemizygous genes that map within the WBS deletion, 14 HSA7q nonhemizygous genes, and 2 genes that map within the LCR flanking the deletion. This panel of genes was completed with 2 HSA7 nonhemizygous genes that map on the short arm of the chromosome (band 7p11.2) and 19 control, non-HSA7 genes. We compared the mRNA expression levels of these genes in nontransformed skin fibroblast cells obtained from 14 subjects with WBS and from 14 controls and in transformed lymphoblastoid cells obtained from 10 subjects with WBS and from 11 controls (see table 1 for cell lines; see table 2 for genotyping²³; and see table 3 for a complete list of assayed genes, primers, and probes).

The results of these analyses are summarized in table 4. We found extensive variability in gene RELs in humans (table 4, fig. 1, and data not shown), which is consistent with previous reports.^{16,17,33} In the population with WBS, all but two of the genes that map to the common deletion interval and that are hemizygous in patients with WBS show average relative expression levels (ARELs) that are approximately half of the normal ARELs (see table 4 and figs. 1C, 1D, and 2), which is consistent with partial results published elsewhere.³⁴ In contrast, the control genes show no significant variation in RELs between the patients and the controls (see table 4 and figs. 1A, 1B, and 2). Interestingly, one hemizygous gene per cell type deviates from

Table 4. ARELs

Gene	Category ^a	Controls		WBS		WBS/Controls			Pairwise <i>t</i> Test <i>P</i>
		AREL	SD	AREL	SD	<i>t</i> Test <i>P</i>	Mann-Whitney <i>P</i>	AREL Ratio ^b	
Lymphoblastoid cell lines:									
<i>GBAS</i>	2	1.38	.37	1.01	.20	.02	.04	.74	...
<i>PSPH</i>	2	1.19	.31	.99	.37	.23	.16	.83	...
<i>ZFD25</i>	2	1.15	.28	.98	.33	.24	.15	.85	...
<i>VKORC1L1</i>	2	1.31	.35	1.05	.42	.15	.15	.80	...
<i>GUSB</i>	2	.95	.18	.92	.36	.82	.35	.97	...
<i>ASL</i>	2	.81	.15	1.29	.39	.004	.004	1.59	...
<i>KCTD7</i>	2	.91	.42	.36	.08	.004	.005	.39	...
<i>NM_017994</i>	2	.99	.19	.89	.14	.18	.13	.89	...
<i>RSAFD1/NM_018264</i>	2	1.13	.23	1.20	.53	.71	.54	1.06	...
<i>AUTS2</i>	2	.57	.50	.20	.21	.06	.06	.35	...
<i>WBSCR20</i>	6	.63	.09	.30	.11	1.0 × 10⁻⁶	.0003	.48	...
<i>TRIM50/73/74</i>	6	1.07	.71	.71	.29	.22	.36	.66	...
<i>BAZ1B</i>	1	2.29	.92	.64	.22	.0006	.0004	.28	...
<i>BCL7B</i>	1	.74	.31	.26	.09	.002	.0004	.35	...
<i>TBL2</i>	1	.64	.14	.24	.08	5.0 × 10⁻⁶	.0003	.38	...
<i>WBSCR24</i>	1	NE	NE	NE	NE	NE	NE	NE	...
<i>WBSCR18</i>	1	NE	NE	NE	NE	NE	NE	NE	...
<i>WBSCR22</i>	1	.65	.20	.28	.09	.0003	.0003	.43	...
<i>STX1A</i>	1	.92	.33	.27	.10	.0003	.0003	.29	...
<i>WBSCR21</i>	1	1.18	.48	.44	.15	.001	.0009	.37	...
<i>CLDN3</i>	1	NE	NE	NE	NE	NE	NE	NE	...
<i>ELN</i>	1	NE	NE	NE	NE	NE	NE	NE	...
<i>LIMK1</i>	1	2.24	.80	.42	.14	.0001	.0004	.19	...
<i>WBSCR1/EIF4H</i>	1	.73	.15	.25	.09	1.1 × 10⁻⁶	.0003	.34	...
<i>WBSCR5</i>	1	.68	.21	.24	.07	.0001	.0003	.36	...
<i>RFC2</i>	1	.86	.28	.40	.12	.0009	.0003	.46	...
<i>CYLN2</i>	1	.81	.37	.23	.08	.001	.0003	.29	...
<i>GTF2IRD1</i>	1	.28	.21	.32	.19	.68	.65	1.14	...
<i>GTF2I</i>	1	.95	.19	.35	.11	2.0 × 10⁻⁶	.0003	.37	...
<i>HIP1</i>	2	.90	.46	.42	.17	.015	.02	.47	...
<i>RHBDL7/NPD007</i>	2	.62	.23	.50	.20	.23	.31	.80	...
<i>POR</i>	2	.56	.14	.50	.15	.37	.71	.89	...
<i>MDH2</i>	2	.86	.08	1.05	.14	.002	.005	1.23	...
<i>DTX2</i>	2	.78	.29	.83	.17	.62	.18	1.07	...
<i>CACNA2D1</i>	2	NE	NE	NE	NE	NE	NE	NE	...
<i>USP18</i>	C	1.19	.71	1.32	.62	.26	.66	1.11	...
<i>DGCR8</i>	C	NE	NE	NE	NE	NE	NE	NE	...
<i>ATP50</i>	C	.45	.11	.47	.16	.71	.21	1.05	...
<i>B2M</i>	C	.63	.12	.60	.28	.76	.54	.95	...
<i>DSCR2</i>	C	1.58	.59	1.99	.95	.29	.45	1.25	...
<i>IFNAR1</i>	C	1.08	.33	1.34	.66	.28	.54	1.25	...
<i>BTG3</i>	C	.79	.25	.56	.19	.04	.02	.71	...
<i>IFNGR2</i>	C	NE	NE	NE	NE	NE	NE	NE	...
<i>GABPA</i>	C	NE	NE	NE	NE	NE	NE	NE	...
<i>IL10RB</i>	C	.94	.11	1.19	.65	.24	.65	1.28	...
<i>SON</i>	C	1.00	.26	.86	.27	.26	.49	.86	...
<i>SIM2</i>	C	1.04	.47	.81	.55	.35	.31	.78	...
<i>UFD1L</i>	C	1.51	.49	1.84	.40	.04	.08	1.22	...
Nonhemizygous:									
All ^c	2	.89	.23	.78	.3588	.20
Centromere ^c	2	.98	.23	.86	.3988	.32
Telomere	2	.74	.14	.66	.2789	.51
Close ^d	2	.81	.23	.58	.3471	.04
LCRs	6	.85	.30	.51	.2960	.03
Hemizygous	1	1.00	.60	.33	.1233	.0005
Controls	C	1.00	.34	1.12	.51	1.12	.16
Skin fibroblasts:									
<i>GBAS</i>	2	.99	.35	.91	.23	.53	.89	.92	...
<i>PSPH</i>	2	.94	.34	.76	.32	.18	.31	.80	...
<i>ZFD25</i>	2	.90	.37	.78	.38	.45	.34	.87	...

(continued)

Table 4. (continued)

Gene	Category ^a	Controls		WBS		WBS/Controls			Pairwise <i>t</i> Test <i>P</i>
		AREL	SD	AREL	SD	<i>t</i> Test <i>P</i>	Mann-Whitney <i>P</i>	AREL Ratio ^b	
<i>VKORC1L1</i>	2	1.10	.33	1.00	.41	.55	.67	.92	...
<i>GUSB</i>	2	.95	.31	1.06	.16	.29	.31	1.11	...
<i>ASL</i>	2	1.11	.32	.85	.23	.03	.08	.77	...
<i>KCTD7</i>	2	.87	.43	.59	.13	.06	.13	.68	...
<i>NM_017994</i>	2	1.09	.24	1.02	.17	.44	.69	.94	...
<i>RSAFD1/NM_018264</i>	2	.98	.19	.93	.16	.50	.47	.95	...
<i>AUTS2</i>	2	1.02	.46	.72	.43	.11	.13	.70	...
<i>WBSCR20</i>	6	.54	.21	.26	.04	.002	.0005	.48	...
<i>TRIM50/73/74</i>	6	NE	NE	NE	NE	NE	NE	NE	...
<i>BAZ1B</i>	1	1.02	.34	.31	.15	8.5 × 10⁻⁶	.00001	.31	...
<i>BCL7B</i>	1	.95	.37	.27	.06	4.6 × 10⁻⁵	.00001	.28	...
<i>TBL2</i>	1	.91	.30	.30	.08	1.7 × 10⁻⁵	.0001	.32	...
<i>WBSCR24</i>	1	.62	.45	.18	.04	.006	.0001	.29	...
<i>WBSCR18</i>	1	1.02	.33	.34	.13	9.9 × 10⁻⁶	.00001	.34	...
<i>WBSCR22</i>	1	.92	.22	.29	.07	3.9 × 10⁻⁷	.00001	.32	...
<i>STX1A</i>	1	.98	.59	.22	.06	.001	.0001	.23	...
<i>WBSCR21</i>	1	.92	.33	.27	.08	1.9 × 10⁻⁵	.0001	.29	...
<i>CLDN3</i>	1	.81	.56	.38	.17	.03	.04	.47	...
<i>ELN</i>	1	1.60	1.63	1.74	1.74	.85	.62	1.08	...
<i>LIMK1</i>	1	.94	.21	.26	.11	2.5 × 10⁻⁸	.00001	.28	...
<i>WBSCR1/EIF4H</i>	1	.91	.31	.28	.08	1.5 × 10⁻⁵	.00001	.30	...
<i>WBSCR5</i>	1	1.15	.48	.38	.12	.0001	.0001	.33	...
<i>RFC2</i>	1	.65	.24	.17	.06	2.4 × 10⁻⁵	.00001	.27	...
<i>CYLN2</i>	1	.61	.19	.18	.05	6.7 × 10⁻⁶	.00001	.29	...
<i>GTF2IRD1</i>	1	.69	.27	.16	.04	3.2 × 10⁻⁵	.00001	.24	...
<i>GTF2I</i>	1	1.36	.38	.72	.18	8.3 × 10⁻⁵	.0001	.53	...
<i>HIP1</i>	2	.51	.29	.29	.09	.03	.04	.56	...
<i>RHBDL7/NPD007</i>	2	.88	.38	.64	.17	.06	.10	.73	...
<i>POR</i>	2	.81	.23	.50	.10	.0006	.005	.62	...
<i>MDH2</i>	2	1.09	.18	.90	.16	.01	.01	.83	...
<i>DTX2</i>	2	1.06	.27	.95	.20	.29	.44	.90	...
<i>CACNA2D1</i>	2	1.01	.61	.94	.62	.80	.98	.94	...
<i>USP18</i>	C	1.05	.55	1.24	.47	.36	.21	1.18	...
<i>DGCR8</i>	C	.98	.63	.94	.32	.83	.84	.95	...
<i>ATP50</i>	C	NE	NE	NE	NE	NE	NE	NE	...
<i>B2M</i>	C	1.07	.57	1.15	.35	.67	.29	1.08	...
<i>DSCR2</i>	C	.87	.26	.80	.28	.53	.56	.92	...
<i>IFNAR1</i>	C	.85	.45	.82	.20	.42	.49	.97	...
<i>BTG3</i>	C	.86	.44	.60	.21	.08	.09	.69	...
<i>IFNGR2</i>	C	.93	.27	.85	.22	.41	.56	.91	...
<i>GABPA</i>	C	1.11	.57	1.37	.61	.30	.31	1.23	...
<i>IL10RB</i>	C	1.03	.40	1.25	.29	.15	.10	1.21	...
<i>SON</i>	C	.61	.24	.43	.10	.03	.03	.71	...
<i>SIM2</i>	C	NE	NE	NE	NE	NE	NE	NE	...
<i>UFD1L</i>	C	NE	NE	NE	NE	NE	NE	NE	...
Nonhemizygous:									
All ^c	2	.96	.16	.80	.2384	.0003
Centromere ^c	2	1.00	.09	.87	.1787	.03
Telomere	2	.89	.22	.71	.2879	.004
Close ^d	2	.94	.19	.74	.2478	.0001
LCRs	6	.54	.21	.26	.0448	.002
Hemizygous	1	.94	.26	.38	.3740	7.3 × 10⁻⁹
Controls	C	.94	.15	.95	.30	1.01	.87

NOTE.—NE indicates that the gene is not expressed in this cell line.

^a 1 = HSA7 hemizygous in WBS; 2 = HSA7 nonhemizygous in WBS; 6 = genes mapping in the LCR flanking the WBS commonly deleted region (i.e., present in six copies/genome); C = control genes.

^b Ratio of ARELs of patients with WBS compared with controls.

^c Does not take into account *GBAS* and *PSPH*, the two genes mapping to the HSA7 short arm.

^d Close nonhemizygous genes on both the centromeric and the telomeric side.

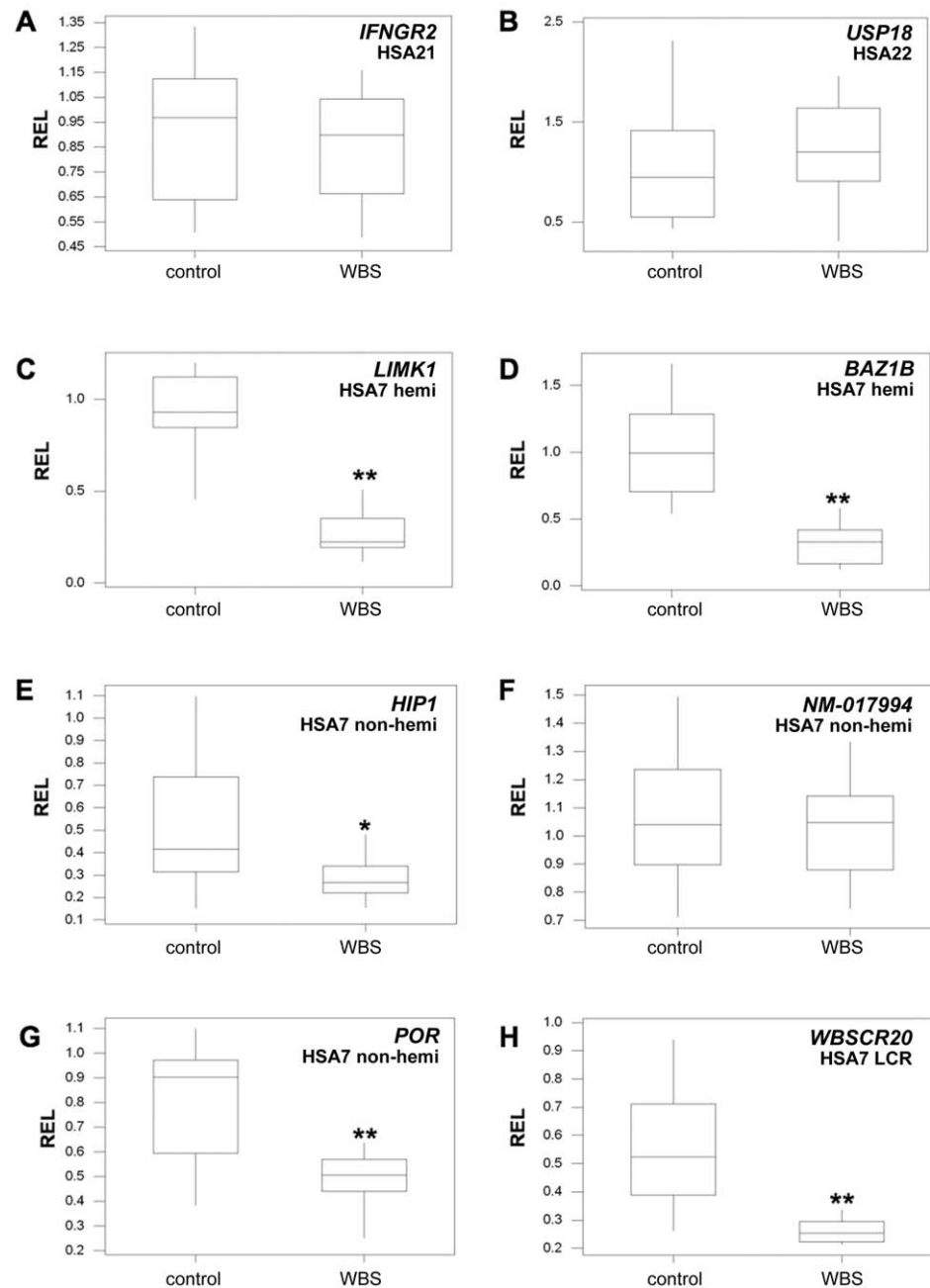


Figure 1. REL distributions measured in 14 patients with WBS and in 14 control skin fibroblasts. REL boxplots are shown for control genes (*IFNGR2* [A] and *USP18* [B]), for hemizygous genes that map to the commonly deleted WBS interval (*LIMK1* [C] and *BAZ1B* [D]), for nonhemizygous genes that map to the flank of the commonly deleted WBS interval (*HIP1* [E], *NM_017994* [F], and *POR* [G]), and for LCR genes that map to the repeats flanking the WBS deletion (*WBSR20* [H]). Asterisks indicate $P < .04$ and double asterisks indicate $P < .005$, at both t and Mann-Whitney tests.

this general pattern; the *GTF2IRD1* gene in lymphoblastoid cells and the *ELN* gene in fibroblasts show no significant changes in their ARELs between control and patient samples.

ELN haploinsufficiency has been linked to supravalvular aortic stenosis (SVAS) and to other stenoses.^{35–39} Here, we find that the REL of the *ELN* gene in skin fibroblasts is

not significantly different between the control population and the patients with WBS ($AREL_{\text{fibro}} = 1.08 \pm 0.31$; $P = .85$) (table 4). This result is in agreement with those obtained using microarray technology (A. Quattrone and G. Merla, unpublished data) but differs substantially from the one described elsewhere.⁴⁰ This discrepancy might be due to the very limited number (only one) of samples

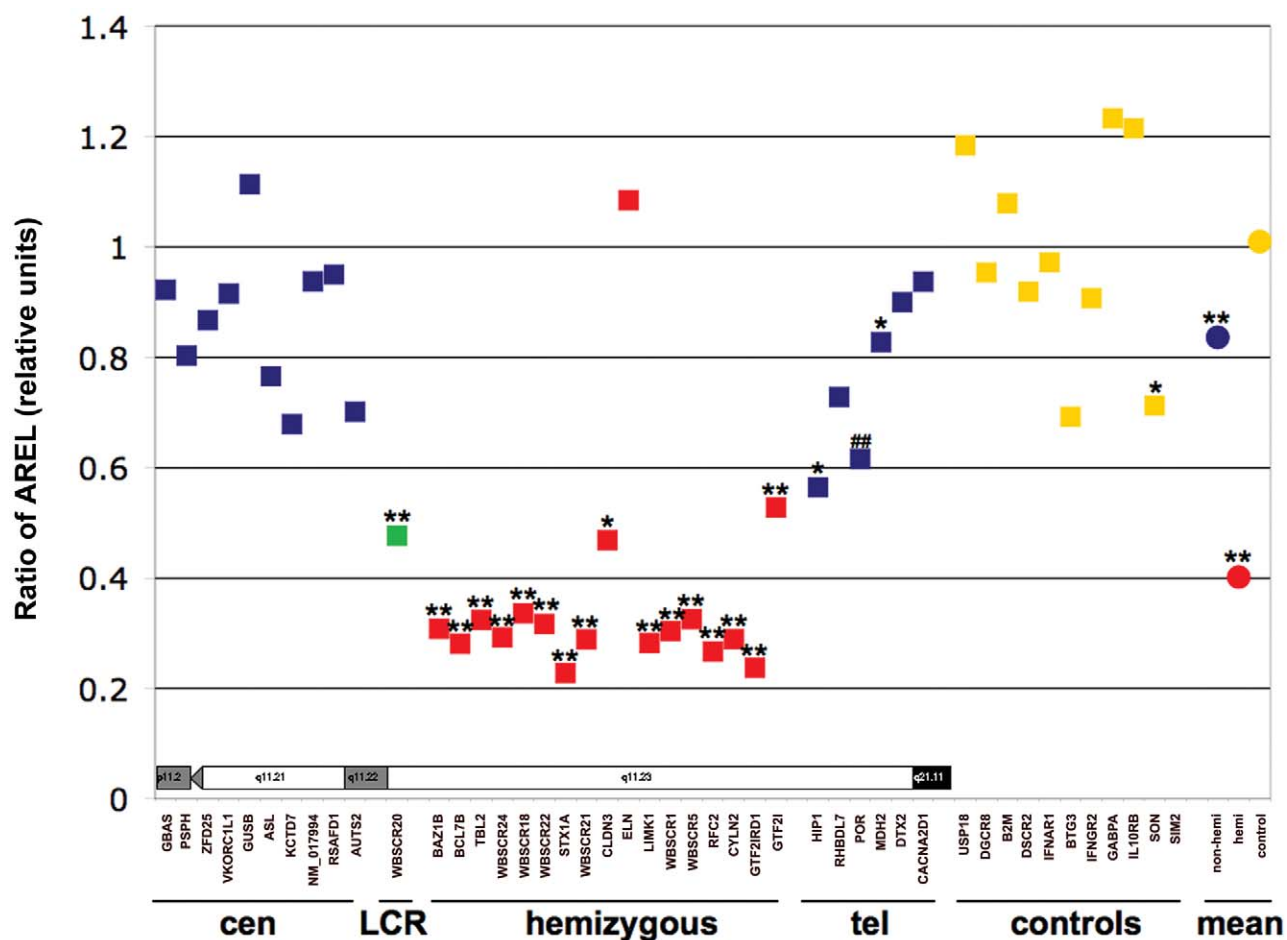


Figure 2. Differences of expression levels in patients with WBS and in controls. Ratio of ARELs from 14 patients with WBS and from 14 controls, measured in skin fibroblasts. *Left to right*, Two HSA7 short-arm genes, HSA7 long-arm genes from the centromere to the telomere, followed by the control genes (*squares*) and the mean (*disks*) of each tested gene category. Nonhemizygous WBS HSA7 genes (*blue*) map centromerically (*cen*) or telomerically (*tel*) of the deletion. LCR = Gene mapping to the repeats flanking the WBS deletion (*green*). hemizygous = Hemizygous WBS HSA7 genes (*red*). controls = Control genes mapping outside HSA7 (*yellow*). A schematic representation (not to scale) of the HSA7 cytogenetic bands in which the assessed genes map is presented in the lower part of the graph. Asterisks indicate $P < .05$ and double asterisks indicate $P < .001$, at both t and Mann-Whitney tests for individual genes and also at pairwise t test for categories. A double number sign (##) indicates that the t and Mann-Whitney tests are significant at $P < .001$ and $P < .005$, respectively (see table 4 for details).

studied and/or to the less sensitive method used in the latter study.⁴⁰ As demonstrated by the large SD (table 4), we observe a large variation in relative expression of *ELN* in the patients with WBS. It is, therefore, possible that the incomplete penetrance of the SVAS phenotype is correlated with the REL of *ELN*^{41,42}—that is, that patients who are under a compensatory mechanism of expression are less likely to present the phenotype. Consistently, the AREL of the *ELN* gene in patients with WBS with SVAS (AREL = 1.15 ± 1.08) is lower than it is in patients with WBS without this phenotype (AREL = 2.56 ± 1.97); however, this difference is not significant. To confirm this hypothesis, we will need to measure the relative expression of this gene in a large number of patients.

A mouse model and recent functional data suggest that

hemizygosity of *CYLN2* and *WBSR14* might contribute to the cognitive profile and to impaired glucose tolerance or silent diabetes, respectively, in patients with WBS.^{43–46} Whereas the study of patients with WBS with atypical deletion suggests that hemizygosity of *GTF2IRD1* and *GTF2I* is linked to their visual spatial processing deficits,^{23–29,47,48} *Gtf2ird1*-null mice display craniofacial abnormalities, thus suggesting a possible link between hemizygosity of *GTF2IRD1* and craniofacial abnormalities displayed in

Table 5. Numbers of UniGene ESTs for TRIM50 and WBSR20

The table is available in its entirety in the online edition of *The American Journal of Human Genetics*.

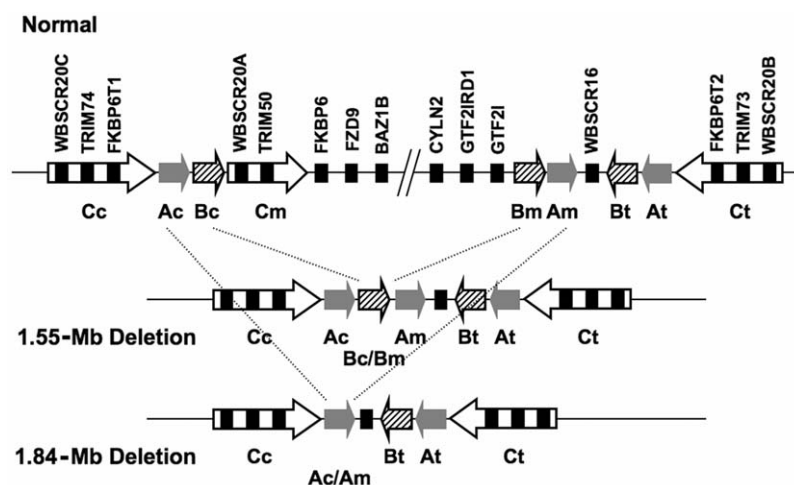


Figure 3. Schematic partial transcript map of the 7q11.23 region in normal chromosome (*top*) and in chromosomes bearing the classical WBS 1.55-Mb (*center*) and 1.84-Mb (*bottom*) deletions. The different centromeric (c), middle (m), and telomeric (t) duplicons within the LCRs are represented by specific arrows that specify their relative orientation and type. Gray arrow indicates BLOCK-A (A); striped arrow indicates BLOCK-B (B); and white arrow indicates BLOCK-C (C). Genes are depicted by black rectangles, with their names given above.

patients with WBS.⁴⁹ In this article, we find that the relative expression of *GTF2IRD1* is significantly decreased in the fibroblasts of patients with WBS ($AREL^{fibro} = 0.24 \pm 0.02$; $P = 3.2 \times 10^{-5}$) but is not affected in lymphoblastoid cell lines ($AREL^{lympho} = 1.14 \pm 0.21$; $P = .68$) (table 4). Thus, we cannot assess the contribution of the *GTF2IRD1* gene to the WBS cognitive phenotype, because its expression might be under special control in the CNS of patients with WBS.

Remarkably, a significant decrease in relative expression was observed for the nonhemizygous genes *ASL*, *KCTD7*, *HIP1*, *POR*, and *MDH2*, which map outside the common deletion region (see table 4 and figs. 1E–1G and 2), although the decrease was not as large as that observed for hemizygous genes. This decrease is significant even if we consider all the tested nonhemizygous genes in fibroblasts mapping to HSA7q or the subset of closest-tested hemizygous genes in lymphoblastoid cells (table 4 and fig. 2).

Two of the tested genes, *WBSCR20* and *TRIM50*, map in the LCRs. Three highly similar copies (*WBSCR20A*, *WBSCR20B*, and *WBSCR20C* and *TRIM50*, *TRIM73*, and *TRIM74*; >98% identity each) of each of these genes are present within the studied region (see table 3 and fig. 3).⁵⁰ *TRIM50* (also known as “*TRIM50A*”) and *WBSCR20A* map centromerically to *FKBP6* within repeat BLOCK-C-mid; *TRIM73* (also known as “*TRIM50B*”) and *WBSCR20B* map telomerically to *FKBP6T2* in BLOCK-C-tel; whereas *TRIM74* (also known as “*TRIM50C*”) and *WBSCR20C* map to the BLOCK-C-cen interval centromeric to *FKBP6T1* (see schematic representation in fig. 3).^{50–52} *WBSCR20A* and *TRIM50*, only one copy of each gene, are hemizygous in patients with WBS (fig. 3).¹⁸ We designed a Taqman assay able to simultaneously recognize all three copies and col-

lectively measure the RELs of all copies. Both *WBSCR20A/B/C* and *TRIM50/73/74* exhibit RELs decreased by about one-half and one-third, respectively, in patients with WBS (see table 4 and figs. 1H and 2), a result that deviates noticeably from the theoretically predicted decrease of 17%. It is possible that different levels of expression of the three copies account for this discrepancy. Consistently, the study of UniGene clusters suggests that *TRIM50* is expressed more than *TRIM73* and *TRIM74* together. Conversely, *WBSCR20A* is not expressed at a higher level than the B and C copies (table 5). These observations suggest that the decrease in relative expression cannot be explained solely by copy-specific expression-level differences. A possible explanation would be that the number of BLOCK-C repeats is polymorphic in the population; however, published results suggest only that the number of BLOCK-A and BLOCK-B copies are polymorphic (see fig. 3).^{52,53} Thus, our results are consistent with the hypothesis that the nondeleted copies in *cis* with the deletion are possibly affected in their expression.

Discussion

Our results suggest that, in genomic disorders, not only the aneuploid genes but also the normal-copy genes that map close to a deletion should be considered as candidate genes for features of these abnormal phenotypes, although we cannot exclude the possibility that what we observe here is only a 7q11.23 region-specific phenomenon. For example, the *HIP1*, *POR*, and *KCTD7* genes, located at distances of 0.7, 1.2, and 6.5 Mb from the WBS region, respectively (table 1), show significantly dysregulated patterns (*t* test $P = .015$ and $P = .025$, $P = 6.3 \times 10^{-4}$, and

$P = 3.8 \times 10^{-3}$, respectively; Mann-Whitney test $P = .025$ and $P = .04$, $P = 5.1 \times 10^{-3}$, and $P = 4.7 \times 10^{-3}$, respectively) (table 4) and are thus good candidates for involvement in certain WBS phenotypic features. Remarkably, it appears that this deregulation is more pronounced for genes mapping closer to the breakpoint (fig. 2). This finding also suggests the presence of very distant long-range *cis*-regulatory elements—to an extent, undescribed elsewhere—and substantiates the notion that functional gene domains extend way beyond their transcription units.⁵⁴ Although this phenomenon was observed in both a transformed and an untransformed cell line, we cannot be certain that the relative expression pattern is the same in the tissues affected with the different phenotypes. However, data obtained elsewhere, from partial Down syndrome mouse models, have shown that relative expression from aneuploid genes is significantly similar across different tissues and developmental stages.^{10,11}

Even though deletions or duplications of large genomic regions result in significant gene expression changes, our results show that the changes are not always directly correlated to copy number, which suggests an underlying complexity that might involve the size of the deletion, the altered structure of chromatin, a dosage-compensation mechanism, or a combination of these factors. In particular, we identified two transcripts within the commonly deleted WBS region for which there were no significant expression differences. Our observations also suggest that changes in the expression levels of genes neighboring large-scale copy-number polymorphisms^{2,3,55–57} might play an important role in phenotypic variation in normal populations and, possibly, in evolution.

Acknowledgments

We thank B. Conrad, E. T. Dermitzakis, S. Deutsch, P. Descombes, M. Docquier, M. Gagnebin, C. Gehrig, H. Kaessmann, C. Ucla, and the members of the GRIEG (Group Interdisciplinaire pour l'étude de l'élastine et son gene) group, for assistance and/or critical reading of the manuscript, and A. Quattrone, for sharing unpublished data. This work was supported by grants from Telathon Action Suisse, the Jérôme Lejeune Foundation, the Désirée and Niels Yde Foundation, the Novartis Foundation, the Swiss National Science Foundation (to A.R.), the European Commission (grant number 037627) (to S.E.A. and A.R.), and the Italian Ministry of Health (to G.M.).

Web Resources

Accession numbers and URLs for data presented herein are as follows:

Coriell Institute for Medical Research, <http://www.coriell.org/index.php/content/view/31/78/> (for cell lines)
 Galliera Genetic Bank, <http://ggb.galliera.it> (for cell lines)
 geNorm, <http://medgen.ugent.be/~jvdesomp/genorm/> (for selection of normalization genes)
 Online Mendelian Inheritance in Man (OMIM), <http://www.ncbi.nlm.nih.gov/Omim/> (for WBS)
 UniGene, <http://www.ncbi.nlm.nih.gov/entrez/query.fcgi?db=>

unigene (for sets of transcript sequences that appear to come from the same transcription locus)

References

- Shaw CJ, Lupski JR (2004) Implications of human genome architecture for rearrangement-based disorders: the genomic basis of disease. *Hum Mol Genet* 13:R57–R64
- Sebat J, Lakshmi B, Troge J, Alexander J, Young J, Lundin P, Maner S, Massa H, Walker M, Chi M, Navin N, Lucito R, Healy J, Hicks J, Ye K, Reiner A, Gilliam TC, Trask B, Patterson N, Zetterberg A, Wigler M (2004) Large-scale copy number polymorphism in the human genome. *Science* 305:525–528
- Iafraite AJ, Feuk L, Rivera MN, Listewnik ML, Donahoe PK, Qi Y, Scherer SW, Lee C (2004) Detection of large-scale variation in the human genome. *Nat Genet* 36:949–951
- Frazer KA, Chen X, Hinds DA, Pant PV, Patil N, Cox DR (2003) Genomic DNA insertions and deletions occur frequently between humans and nonhuman primates. *Genome Res* 13:341–346
- Liu G, Zhao S, Bailey JA, Sahinalp SC, Alkan C, Tuzun E, Green ED, Eichler EE (2003) Analysis of primate genomic variation reveals a repeat-driven expansion of the human genome. *Genome Res* 13:358–368
- Locke DP, Seagraves R, Carbone L, Archidiacono N, Albertson DG, Pinkel D, Eichler EE (2003) Large-scale variation among human and great ape genomes determined by array comparative genomic hybridization. *Genome Res* 13:347–357
- Koszul R, Caburet S, Dujon B, Fischer G (2004) Eucaryotic genome evolution through the spontaneous duplication of large chromosomal segments. *EMBO J* 23:234–243
- Khaitovich P, Muetzel B, She X, Lachmann M, Hellmann I, Dietzsch J, Steigele S, Do HH, Weiss G, Enard W, Heissig F, Arendt T, Nieselt-Struwe K, Eichler EE, Paabo S (2004) Regional patterns of gene expression in human and chimpanzee brains. *Genome Res* 14:1462–1473
- Muller S, Finelli P, Neusser M, Wienberg J (2004) The evolutionary history of human chromosome 7. *Genomics* 84:458–467
- Lyle R, Gehrig C, Neergaard-Henrichsen C, Deutsch S, Antonarakis SE (2004) Gene expression from the aneuploid chromosome in a trisomy mouse model of down syndrome. *Genome Res* 14:1268–1274
- Kahlem P, Sultan M, Herwig R, Steinfath M, Balzereit D, Eppens B, Saran NG, Pletcher MT, South ST, Stetten G, Lehrach H, Reeves RH, Yaspo ML (2004) Transcript level alterations reflect gene dosage effects across multiple tissues in a mouse model of down syndrome. *Genome Res* 14:1258–1267
- Amano K, Sago H, Uchikawa C, Suzuki T, Kotliarova SE, Nukina N, Epstein CJ, Yamakawa K (2004) Dosage-dependent over-expression of genes in the trisomic region of Ts1Cje mouse model for Down syndrome. *Hum Mol Genet* 13:1333–1340
- Hollox EJ, Armour JA, Barber JC (2003) Extensive normal copy number variation of a β -defensin antimicrobial-gene cluster. *Am J Hum Genet* 73:591–600
- Lettice LA, Heaney SJ, Purdie LA, Li L, de Beer P, Oostra BA, Goode D, Elgar G, Hill RE, de Graaff E (2003) A long-range Shh enhancer regulates expression in the developing limb and fin and is associated with preaxial polydactyly. *Hum Mol Genet* 12:1725–1735
- Spitz F, Gonzalez F, Duboule D (2003) A global control region

- defines a chromosomal regulatory landscape containing the HoxD cluster. *Cell* 113:405–417
16. Morley M, Molony CM, Weber TM, Devlin JL, Ewens KG, Spielman RS, Cheung VG (2004) Genetic analysis of genome-wide variation in human gene expression. *Nature* 430:743–747
 17. Cheung VG, Spielman RS, Ewens KG, Weber TM, Morley M, Burdick JT (2005) Mapping determinants of human gene expression by regional and genome-wide association. *Nature* 437:1365–1369
 18. Bayes M, Magano LF, Rivera N, Flores R, Perez Jurado LA (2003) Mutational mechanisms of Williams-Beuren syndrome deletions. *Am J Hum Genet* 73:131–151
 19. Morris CA, Demsey SA, Leonard CO, Dilts C, Blackburn BL (1988) Natural history of Williams syndrome: physical characteristics. *J Pediatr* 113:318–326
 20. Francke U (1999) Williams-Beuren syndrome: genes and mechanisms. *Hum Mol Genet* 8:1947–1954
 21. Osborne LR (1999) Williams-Beuren syndrome: unraveling the mysteries of a microdeletion disorder. *Mol Genet Metab* 67:1–10
 22. Stromme P, Bjornstad PG, Ramstad K (2002) Prevalence estimation of Williams syndrome. *J Child Neurol* 17:269–271
 23. Howald C, Merla G, Digilio MC, Amenta S, Lyle R, Deutsch S, Choudhury U, Bottani A, Antonarakis SE, Fryssira H, Dallapiccola B, Reymond A (2006) Two high throughput technologies to detect segmental aneuploidies identify new Williams-Beuren syndrome patients with atypical deletions. *J Med Genet* 43:266–273
 24. Korenberg JR, Chen XN, Hirota H, Lai Z, Bellugi U, Burian D, Roe B, Matsuoka R (2000) VI. Genome structure and cognitive map of Williams syndrome. *J Cogn Neurosci* 12:89–107
 25. Hirota H, Matsuoka R, Chen XN, Salandanan LS, Lincoln A, Rose FE, Sunahara M, Osawa M, Bellugi U, Korenberg JR (2003) Williams syndrome deficits in visual spatial processing linked to GTF2IRD1 and GTF2I on chromosome 7q11.23. *Genet Med* 5:311–321
 26. Gagliardi C, Bonaglia MC, Selicorni A, Borgatti R, Giorda R (2003) Unusual cognitive and behavioural profile in a Williams syndrome patient with atypical 7q11.23 deletion. *J Med Genet* 40:526–530
 27. Botta A, Novelli G, Mari A, Novelli A, Sabani M, Korenberg J, Osborne LR, Digilio MC, Giannotti A, Dallapiccola B (1999) Detection of an atypical 7q11.23 deletion in Williams syndrome patients which does not include the STX1A and FZD3 genes. *J Med Genet* 36:478–480
 28. Heller R, Rauch A, Luttgen S, Schroder B, Winterpacht A (2003) Partial deletion of the critical 1.5 Mb interval in Williams-Beuren syndrome. *J Med Genet* 40:e99
 29. Morris CA, Mervis CB, Hobart HH, Gregg RG, Bertrand J, Ensing GJ, Sommer A, Moore CA, Hopkin RJ, Spallone PA, Keating MT, Osborne L, Kimberley KW, Stock AD (2003) GTF2I hemizyosity implicated in mental retardation in Williams syndrome: genotype-phenotype analysis of five families with deletions in the Williams syndrome region. *Am J Med Genet A* 123:45–59
 30. Osborne LR, Li M, Pober B, Chitayat D, Bodurtha J, Mandel A, Costa T, Grebe T, Cox S, Tsui LC, Scherer SW (2001) A 1.5 million-base pair inversion polymorphism in families with Williams-Beuren syndrome. *Nat Genet* 29:321–325
 31. Livak KJ, Schmittgen TD (2001) Analysis of relative gene expression data using real-time quantitative PCR and the $2^{-\Delta\Delta C_t}$ method. *Methods* 25:402–408
 32. Vandesompele J, De Preter K, Pattyn F, Poppe B, Van Roy N, De Paepe A, Speleman F (2002) Accurate normalization of real-time quantitative RT-PCR data by geometric averaging of multiple internal control genes. *Genome Biol* 3:RESEARCH0034
 33. Deutsch S, Lyle R, Dermitzakis ET, Attar H, Subrahmanyam L, Gehrig C, Parand L, Gagnebin M, Rougemont J, Jongeneel CV, Antonarakis SE (2005) Gene expression variation and expression quantitative trait mapping of human chromosome 21 genes. *Hum Mol Genet* 14:3741–3749
 34. Somerville MJ, Mervis CB, Young EJ, Seo EJ, del Campo M, Bamforth S, Peregrine E, Loo W, Lilley M, Perez-Jurado LA, Morris CA, Scherer SW, Osborne LR (2005) Severe expressive-language delay related to duplication of the Williams-Beuren locus. *N Engl J Med* 353:1694–1701
 35. Ewart AK, Morris CA, Atkinson D, Jin W, Sternes K, Spallone P, Stock AD, Leppert M, Keating MT (1993) Hemizyosity at the elastin locus in a developmental disorder, Williams syndrome. *Nat Genet* 5:11–16
 36. Curran ME, Atkinson DL, Ewart AK, Morris CA, Leppert MF, Keating MT (1993) The elastin gene is disrupted by a translocation associated with supravalvular aortic stenosis. *Cell* 73:159–168
 37. Tassabehji M, Metcalfe K, Donnai D, Hurst J, Reardon W, Burch M, Read AP (1997) Elastin: genomic structure and point mutations in patients with supravalvular aortic stenosis. *Hum Mol Genet* 6:1029–1036
 38. Li DY, Brooke B, Davis EC, Mecham RP, Sorensen LK, Boak BB, Eichwald E, Keating MT (1998) Elastin is an essential determinant of arterial morphogenesis. *Nature* 393:276–280
 39. Li DY, Faury G, Taylor DG, Davis EC, Boyle WA, Mecham RP, Stenzel P, Boak B, Keating MT (1998) Novel arterial pathology in mice and humans hemizygous for elastin. *J Clin Invest* 102:1783–1787
 40. Urban Z, Michels VV, Thibodeau SN, Davis EC, Bonnefont JP, Munnich A, Eyskens B, Gewillig M, Devriendt K, Boyd CD (2000) Isolated supravalvular aortic stenosis: functional haploinsufficiency of the elastin gene as a result of nonsense-mediated decay. *Hum Genet* 106:577–588
 41. Pankau R, Siebert R, Kautza M, Schneppenheim R, Gosch A, Wessel A, Partsch CJ (2001) Familial Williams-Beuren syndrome showing varying clinical expression. *Am J Med Genet* 98:324–329
 42. Wang MS, Schinzel A, Kotzot D, Balmer D, Casey R, Chodirker BN, Gyftodimou J, Petersen MB, Lopez-Rangel E, Robinson WP (1999) Molecular and clinical correlation study of Williams-Beuren syndrome: no evidence of molecular factors in the deletion region or imprinting affecting clinical outcome. *Am J Med Genet* 86:34–43
 43. Cairo S, Merla G, Urbinati F, Ballabio A, Reymond A (2001) WBSR14, a gene mapping to the Williams-Beuren syndrome deleted region, is a new member of the Mlx transcription factor network. *Hum Mol Genet* 10:617–627
 44. Hoogenraad CC, Koekkoek B, Akhmanova A, Krugers H, Dordland B, Miedema M, van Alphen A, Kistler WM, Jaegle M, Koutsourakis M, Van Camp N, Verhoye M, van der Linden A, Kaverina I, Grosveld F, De Zeeuw CI, Galjart N (2002) Targeted mutation of Cyln2 in the Williams syndrome critical region links CLIP-115 haploinsufficiency to neurodevelopmental abnormalities in mice. *Nat Genet* 32:116–127

45. Iizuka K, Bruick RK, Liang G, Horton JD, Uyeda K (2004) Deficiency of carbohydrate response element-binding protein (ChREBP) reduces lipogenesis as well as glycolysis. *Proc Natl Acad Sci USA* 101:7281–7286
46. Merla G, Howald C, Antonarakis SE, Reymond A (2004) The subcellular localization of the ChoRE-binding protein, encoded by the Williams-Beuren syndrome critical region gene 14, is regulated by 14-3-3. *Hum Mol Genet* 13:1505–1514
47. Karmiloff-Smith A, Grant J, Ewing S, Carette MJ, Metcalfe K, Donnai D, Read AP, Tassabehji M (2003) Using case study comparisons to explore genotype-phenotype correlations in Williams-Beuren syndrome. *J Med Genet* 40:136–140
48. Tassabehji M, Metcalfe K, Karmiloff-Smith A, Carette MJ, Grant J, Dennis N, Reardon W, Splitt M, Read AP, Donnai D (1999) Williams syndrome: use of chromosomal microdeletions as a tool to dissect cognitive and physical phenotypes. *Am J Hum Genet* 64:118–125
49. Tassabehji M, Hammond P, Karmiloff-Smith A, Thompson P, Thorgeirsson SS, Durkin ME, Popescu NC, Hutton T, Metcalfe K, Rucka A, Stewart H, Read AP, Maconochie M, Donnai D (2005) GTF2IRD1 in craniofacial development of humans and mice. *Science* 310:1184–1187
50. Merla G, Ucla C, Guipponi M, Reymond A (2002) Identification of additional transcripts in the Williams-Beuren syndrome critical region. *Hum Genet* 110:429–438
51. Doll A, Grzeschik KH (2001) Characterization of two novel genes, WBSCR20 and WBSCR22, deleted in Williams-Beuren syndrome. *Cytogenet Cell Genet* 95:20–27
52. Valero MC, de Luis O, Cruces J, Perez Jurado LA (2000) Fine-scale comparative mapping of the human 7q11.23 region and the orthologous region on mouse chromosome 5G: the low-copy repeats that flank the Williams-Beuren syndrome deletion arose at breakpoint sites of an evolutionary inversion(s). *Genomics* 69:1–13
53. Perez Jurado LA, Wang YK, Peoples R, Coloma A, Cruces J, Francke U (1998) A duplicated gene in the breakpoint regions of the 7q11.23 Williams-Beuren syndrome deletion encodes the initiator binding protein TFII-I and BAP-135, a phosphorylation target of BTK. *Hum Mol Genet* 7:325–334
54. Kleinjan DA, van Heyningen V (2005) Long-range control of gene expression: emerging mechanisms and disruption in disease. *Am J Hum Genet* 76:8–32
55. Bignell GR, Huang J, Greshock J, Watt S, Butler A, West S, Grigorova M, Jones KW, Wei W, Stratton MR, Futreal PA, Weber B, Shapero MH, Wooster R (2004) High-resolution analysis of DNA copy number using oligonucleotide microarrays. *Genome Res* 14:287–295
56. Sharp AJ, Locke DP, McGrath SD, Cheng Z, Bailey JA, Vallente RU, Pertz LM, Clark RA, Schwartz S, Segraves R, Oseroff VV, Albertson DG, Pinkel D, Eichler EE (2005) Segmental duplications and copy-number variation in the human genome. *Am J Hum Genet* 77:78–88
57. Tuzun E, Sharp AJ, Bailey JA, Kaul R, Morrison VA, Pertz LM, Haugen E, Hayden H, Albertson D, Pinkel D, Olson MV, Eichler EE (2005) Fine-scale structural variation of the human genome. *Nat Genet* 37:727–732